Rotation Characteristics of Main Ions and Impurity Ions in *H*-Mode Tokamak Plasma

J. Kim, K. H. Burrell, P. Gohil, R. J. Groebner, Y.-B. Kim, H. E. St. John, R. P. Seraydarian, and M. R. Wade*

General Atomics, San Diego, California 92186

(Received 11 August 1993)

Poloidal and toroidal rotation of the main ions (He^{2+}) and the impurity ions (C^{6+} and B^{5+}) in *H*-mode helium plasmas have been measured via charge exchange recombination spectroscopy in the DIII-D tokamak. It was discovered that the main ion poloidal rotation is in the *ion diamagnetic drift* direction while the impurity ion rotation is in the *electron diamagnetic drift* direction, in qualitative agreement with the neoclassical theory. The deduced radial electric field in the edge is of the same negative-well shape regardless of which ion species is used, validating the fundamental nature of the electric field in *L-H* transition phenomenology.

PACS numbers: 52.55.Fa, 52.55.Pi, 52.70.Kz

Since its original discovery in ASDEX [1], the *H* mode has proven to be one of the most robust and ubiquitous modes of improved confinement in toroidal magnetic fusion devices. The physics of the *L*-mode to *H*-mode (*L-H*) transition has attracted a great deal of interest and effort from both the experimental and theoretical communities. Critical reviews of this subject have recently been made by Burrell *et al.* [2] and Groebner [3]. Although a complete, quantitative theory of the confinement improvement at the *L-H* transition does not yet exist, combined theoretical and experimental work has merged into a paradigm that a highly sheared $\mathbf{E}\times\mathbf{B}$ flow in the plasma edge can lead to better confinement through decorrelation of the fluctuations, decreased radial correlation lengths, and reduced turbulent transport [4,5]. The experimental observations that the edge impurity ion poloidal rotation [6–9] and the edge radial electric field [6–11] change dramatically and abruptly at the *L-H* transition have led to several theories which consider how the radial electric field or the (main) ion poloidal rotation changes across the *L-H* transition. Among these are theories based on bifurcation of the radial electric field [5,12], Stringer spin-up [13,14], turbulent Reynolds stress [15], temperature gradient-induced poloidal rotation [16], and particle and energy confinement bifurcation [17].

Only the impurity ion rotation measurements have been available previously and some theoretical models were developed to explain the sudden (≤ 1 msec) increase of poloidal rotation (in the electron diamagnetic drift direction) at the *L-H* transition; these theories implicitly assumed that the main ion rotation and the impurity ion rotation are identical. However, recent neoclassical derivations of rotation velocities predict that the main ion poloidal rotation and the impurity ion poloidal rotation speed could be quite different [18,19]. Although not in *H* mode, a comparison of the main and the impurity ion poloidal rotation in Ohmic plasmas in TEXT was reported previously [20], which showed little difference between them. Experimental clarification of the rotation behavior of the main and impurity ions in *H*-mode plasmas is important not only as a check of the neoclassical rotation theories, but also as a test of the existing *L-H* transition theories. However, charge exchange recombination (CER) measurement of the main ion rotation is very difficult in neutral beam heated deuterium plasma because the D_α line is usually obscured by large thermal emission from the plasma edge and by Doppler-shifted emission from injected beam neutrals themselves. In addition, spatial resolution is compromised by cross-field thermal motion of the excited deuterium neutrals born via charge exchange.

In this paper, we report the first direct measurement of the main ion poloidal and toroidal rotation characteristics in *H*-mode tokamak plasma. By employing helium plasmas in the DIII-D tokamak and by using CER spectroscopy for the He II, C VI, and B V lines, we have discovered that the *sign* of the poloidal rotation of the main ions and the impurity ions is indeed *opposite*, in agreement with the neoclassical prediction [18], but that the magnitude of the main ion poloidal rotation is much greater than the prediction. The measurement also shows an appreciable difference in toroidal rotation between the main and the impurity ions in the edge region. Implications of the experimental results on *L-H* transition theories and rotation theories will be presented.

The CER system [21–23] on the DIII-D tokamak allows us to monitor any select spectral line emitted from excited ions localized where the line of sight and the neutral beam cross. These spectral lines contain information on the Doppler broadening (temperature) and the Doppler shift (rotation speed). The spatial coverage ranges from $R=1.77$ m to $R=2.30$ m while the magnetic axis is around $R=1.75$ m. The neutral beam injection (NBI) lines are aimed tangentially at the plasma on the median plane [24]. Deuterium NBI was chosen to provide CER for He^{2+} [$He^{2+}+D^0 \rightarrow (He^+)^* + D^+$] and to force the *L-H* transition in helium plasmas. In the case of helium NBI, the He II spectrum was found to be obscured by the light originating from slowing-down fast He^{2+} ions. The

0031-9007/94/72(14)/2199(4)$06.00

NBI was modulated to allow subtraction of the plasma emission (without beam) from the total emission (with beam) to yield pure CER spectra. Carbon and boron are the main impurities in the DIII-D tokamak whose graphite inner wall was *boronized* by means of glow discharge using diborane and helium gas. In addition, D^+ ions from the injected beams are also an impurity in the helium plasma. Comparison of the thermal D-D neutron output in the helium plasma and in a deuterium plasma of similar condition indicates that the ratio of the deuterium density to the electron density is about 10% in the Ohmic phase, and the D^+ content increases with NBI. The unshifted wavelength locations needed for obtaining Doppler shifts were determined by the line locations of the spectra during the Ohmic phase of the shot. Fiducials obtained in this way were validated by using a pair of opposing tangential chords focused at the same major radius point.

Some parameters of interest in the single-null divertor discharges used in this study are $B_\phi = -2$ T, $n_e = (1-4)\times 10^{19}$ m^{-3}, $I_p = 1$ MA, and $P_{\mathrm{inj}} = 5$ MW. The ion collisionality parameter (ν_{ii}^*) ranges from 0.1 to 0.3 in the edge region well after the L-H transition. Photodiode signals show the onset of a dithering L-H transition at around $t = 2330$ ms ($t = 0$ is the start of the discharge) and most analyses were done at around $t = 2480$ ms. In the right hand (r,θ,ϕ) coordinate system, the sign convention of our experiment is as follows: The toroidal magnetic field B_ϕ is *negative* (clockwise viewed from above); the poloidal field B_θ is *positive* (i.e., *downward* at the outboard median); I_p and NBI are in the *positive* toroidal direction; the ion diamagnetic drift direction (ω_{*i} direction) is *positive*; the electron diamagnetic drift direction (ω_{*e} direction) is *negative*.

The neoclassical poloidal rotation of the main ions ($V_{\theta i}$) and the impurity ions ($V_{\theta I}$) are given by [18]

$$V_{\theta i} = \tfrac{1}{2} V_{i\mathrm{th}}\rho_i K_1 L_{T_i}^{-1} \frac{|B| B_\phi}{\langle B^2\rangle}, \qquad (1)$$

$$V_{\theta I} = \tfrac{1}{2} V_{i\mathrm{th}}\rho_i \left\{ (K_1 + \tfrac{3}{2}K_2) L_{T_i}^{-1} - L_{P_i}^{-1} + \frac{Z_i T_I}{Z_I T_i} L_{P_I}^{-1} \right\} \frac{|B| B_\phi}{\langle B^2\rangle}, \qquad (2)$$

where subscripts i and I denote the main ion and the impurity ion, respectively. Complete definitions of the symbols in Eqs. (1) and (2) can be found in Ref. [18]. The pressure scale length (L_{P_i}) is related to the temperature scale length (L_{T_i}) and the density scale length (L_{n_i}) by $L_{P_i}^{-1} = L_{T_i}^{-1} + L_{n_i}^{-1}$, where $L_{T_i}^{-1} = d(\ln T_i)/dr$. L_{T_i} and L_{n_i} are negative because both n_i and T_i typically decrease with r. Both the temperature profiles and the density profiles are obtained from CER spectroscopy. The collisionality parameter (ν^*), needed for K_1 and K_2, is calculated using a generalized definition given in Ref. [18] rather than the usual large aspect-ratio approximation. Local and flux-surface averaged magnetic fields used in the theoretical computation are obtained from MHD equilibrium analysis [25]. $V_{\theta i}$ is typically positive (ω_{*i} direction) since $K_1 > 0$, $L_{T_i}^{-1} < 0$, and $B_\phi < 0$.

Manipulation of Eq. 36 in Ref. [18] shows that the difference of the main and the impurity ion toroidal rotation speed does not depend on the radial electric field. The resulting expression for the difference in toroidal rotation speeds is given below,

$$V_{\phi i} - V_{\phi I} = -\tfrac{1}{2} V_{i\mathrm{th}}\rho_{\theta i} K_2 L_{T_i}^{-1} + \tfrac{1}{2} V_{i\mathrm{th}}\rho_{\theta i}\left(\tfrac{3}{2}K_2 L_{T_i}^{-1} - L_{P_i}^{-1} + \frac{Z_i T_I}{Z_I T_i} L_{P_I}^{-1}\right)\left(1 - \frac{B_\phi^2}{\langle B^2\rangle}\right), \qquad (3)$$

where $\rho_{\theta i}$ is the poloidal gyroradius of the main ion. The right hand side of Eq. (3) can be computed from measured profiles and thus can be directly compared with the measured difference of the toroidal rotation speeds.

The radial electric field is derived from the equilibrium force balance equation. The same equation is also valid for the impurity ion (by changing the subscript from i to I),

$$E_r = \frac{1}{n_i Z_i e}\frac{dP_i}{dr} - V_{\theta i}B_\phi + V_{\phi i}B_\theta, \qquad (4)$$

where $Z_i e$ is the charge of the ion. Since P_i decreases with r, the first term is negative.

Measured poloidal rotation velocities of He^{2+} and C^{6+} in the edge region about 150 ms after the L-H transition are shown in Fig. 1. A clear difference in rotation characteristics between the main and the impurity ions is apparent. The directions of the poloidal rotations are in agreement with the neoclassical predictions [18]. $V_{\theta i}$ is

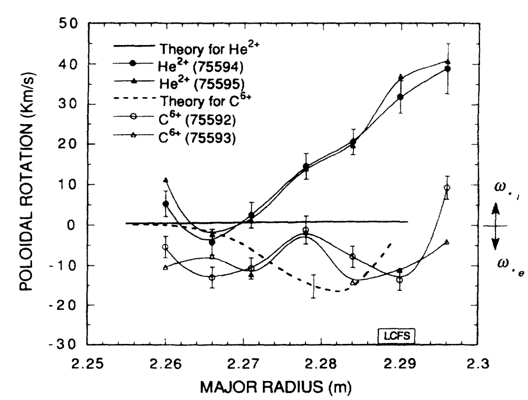

FIG. 1. Measured and calculated poloidal rotation of the main ions (He^{2+}) and the impurity ions (C^{6+}) in the edge region about 150 ms after L-H transition. The LCFS varies somewhat from shot to shot. The error bars represent 1 standard deviation of the random error.

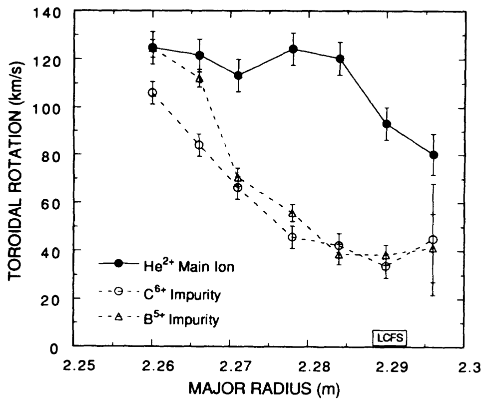

FIG. 2. Measured toroidal rotation of the main (helium) and the impurity (carbon and boron) ions in the edge region.

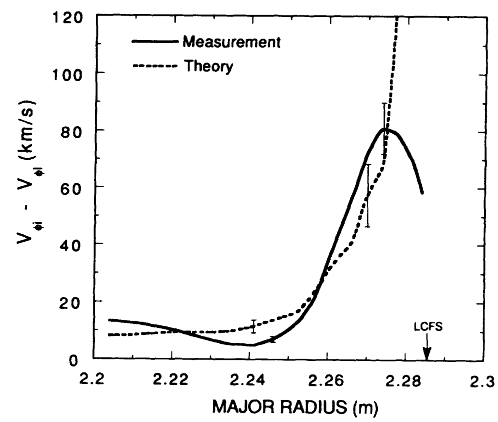

FIG. 3. Comparison of measured and predicted $V_{\phi i}-V_{\phi I}$, where two plasma shots (not exactly corresponding to the ones in Fig. 2) are combined (He^{2+} and C^{6+}).

in the ω_{*i} direction, while $V_{\theta I}$ is in the usual ω_{*e} direction. $V_{\theta I}$ is appreciably slower than $V_{\theta i}$. Neoclassical predictions for $V_{\theta i}$ and $V_{\theta I}$ are also plotted in Fig. 1. It is noted, however, that $L_{n_i}\sim 1$ cm and $\rho_{\theta i}\sim 2$ cm in the region a few cm within the last closed flux surface (LCFS) or the separatrix, and thus the neoclassical theory, which is based on the assumption of $L\gg\rho_{\theta i}$, may *not be valid* there. Although not shown in the figure, $V_{\theta i}$ and $V_{\theta I}$ in Ohmic phase and L-mode phase are small and equal in magnitude and flat in profile.

The measured $V_{\phi i}$ and $V_{\phi I}$ are shown in Fig. 2. They are again different in the edge: $V_{\phi i}$ remains relatively large even around the LCFS whereas $V_{\phi I}$ decreases more rapidly towards the LCFS. It is noted that, although not shown in the figure, $V_{\phi i}$ and $V_{\phi I}$ are quite similar in the core region. In Fig. 3, the measured $V_{\phi i}-V_{\phi I}$ is compared with the prediction [Eq. (3)]. The agreement is relatively good, but discrepancy shows up also in the high shear edge region.

Because E_r is the property of the overall plasma common to any species, one should expect an identical result from all the ion species as computed from Eq. (4). This very fact, therefore, serves also as a consistency check on the experimental results. Shown in Fig. 4 are the E_r profiles inferred from He^{2+}, C^{6+}, and B^{5+}, respectively. Considering the different rotation characteristics of the main ions and the impurity ions, the agreement among the three independent E_r profiles is quite remarkable. For the main ion, a negative well shape of E_r in the edge region is maintained by the dominant pressure gradient term against the positive contribution from the $-V_{\theta i}B_\phi$ and $V_{\phi i}B_\theta$ terms, while for the impurity ion both the pressure gradient term and the $-V_{\theta I}B_\phi$ term are negative against the positive contribution from the $V_{\phi I}B_\theta$ term. It is noteworthy that, given the same gradient scale lengths, the contribution of the pressure gradient term for the impurity is smaller by a factor of Z_i/Z_I than for the main ion. For example, at about 1 cm inside the LCFS, the contributions of the three terms are, in the order given in Eq. (4), -90, 30, 40 kV/m for He^{2+} and -25, -20, 20 kV/m for C^{6+}, respectively.

The temperatures of the main ions (He^{2+}) and the impurity ions (C^{6+} and B^{5+}) are basically identical throughout the plasma cross section as shown in Fig. 5. This is perhaps the first experimental comparison of the main and the impurity ion temperature profiles. In the very edge region, however, there seems to be a small deviation between T_i and T_I, which warrants future investigation.

We now focus our discussion on the implications of the experimental results for L-H transition theories: Several theories [5,13,16] attempt to explain the connection between the L-H transition and the observed sudden jump of $V_{\theta I}$ in the ω_{*e} direction. Since $V_{\theta i}$ is in the ω_{*i} direction, these theories were led to explain the wrong phenomenon. Another important implication is that the E_r consists of three comparable terms and hence the

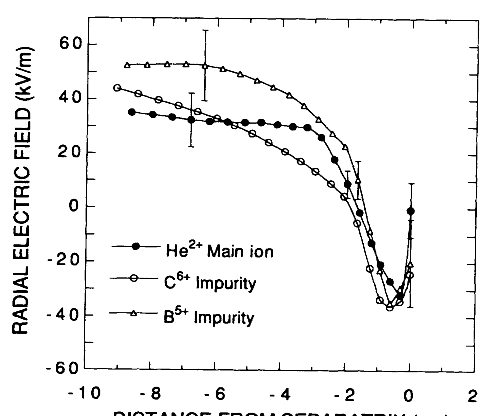

FIG. 4. Radial electric fields deduced from the main ion (helium) and the impurity ion (carbon and boron) measurements as a function of the distance relative to the LCFS.

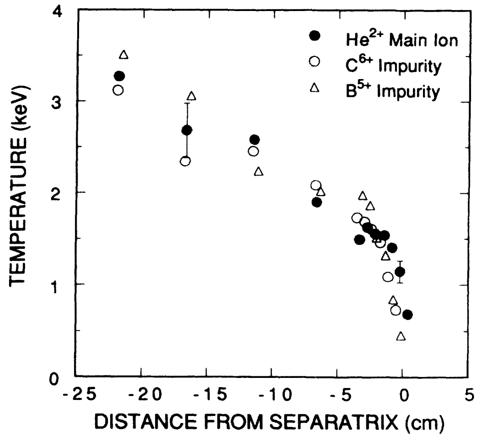

FIG. 5. Comparison of the temperature profiles obtained from He^{2+}, C^{6+}, and B^{5+}.

$\mathbf{E}\times\mathbf{B}$ flow cannot be approximated solely by the main ion poloidal flow. Some theories [4,15] opted not to distinguish the $\mathbf{E}\times\mathbf{B}$ flow and the poloidal rotation. The radial electric field was shown to be the same regardless of which ion species is used to deduce it. Therefore E_r is a more fundamental parameter than the rotation flows themselves. As long as E_r is used in the study of H mode, the impurity ion measurements are as useful as the main ion measurements which are usually much harder to obtain. Hence, L-H transition theories [5,12,15,17] based on the bifurcation of E_r may still be valid. For example, the normalized poloidal rotation parameter (U_{pm}) of Shaing's theory [5] was previously computed from the main ion data to show an agreement with the theory across the L-H transition [2]. This is primarily due to the pressure gradient term. However, the ion orbit loss current, which is the primary driver for the L-H transition in this theory, forces $V_{\theta i}$ to be in the ω_{*e} direction.

Opposite signs of $V_{\theta i}$ and $V_{\theta I}$ are in accord with the neoclassical predictions of poloidal rotation. In the high-shear edge region of the H-mode plasma where poloidal rotation is large, however, the validity of the neoclassical theory breaks down and the prediction is very far off. The prediction for $V_{\theta I}$ is not bad, however. Inclusion of orbit squeezing effects could account for the relatively large main ion poloidal rotation speed there [26]. The predicted difference in the toroidal rotation, $V_{\phi i} - V_{\phi I}$, compares reasonably well with the measurement. Future investigation should be focused on the fine-time-resolved behavior of the main ion rotation and pressure gradient across the L-H transition and over a wider range of collisionality.

We would like to thank our colleagues who helped us in the course of this work, in particular, Dr. D. Hillis, Dr. F. L. Hinton, Dr. R. Hong, Dr. G. L. Jackson, Dr. A. W. Leonard, Dr. W. Mandl, Dr. R. Miller, Dr. G. M. Staebler, Dr. R. D. Stambaugh, and Dr. T. S. Taylor. This work was supported by the Department of Energy under Contracts No. DE-AC03-89ER51114 and No. DE-AC05-84OR21400.

*Permanent address: Oak Ridge National Laboratory, Oak Ridge, Tennessee.

[1] F. Wagner, G. Becker, and K. Behringer *et al.*, Phys. Rev. Lett. **49**, 1408 (1982); F. Wagner, R. Bartiromo, and G. Becker *et al.*, Nucl. Fusion **25**, 1490 (1985).
[2] K. H. Burrell *et al.*, Plasma Phys. Controlled Fusion **34**, 1859 (1992).
[3] R. J. Groebner, Phys. Fluids B **5**, 2343 (1993).
[4] H. Biglari, P. H. Diamond, and P. W. Terry, Phys. Fluids B **2**, 1 (1990).
[5] K. C. Shaing and E. C. Crume, Jr., Phys. Rev. Lett. **63**, 2368 (1989); K. C. Shaing, E. C. Crume, Jr., and W. A. Houlberg, Phys. Fluids B **2**, 1492 (1990).
[6] R. J. Groebner, K. H. Burrell, and R. P. Seraydarian, Phys. Rev. Lett. **64**, 3015 (1990).
[7] R. J. Groebner, W. A. Peebles, and K. H. Burrell *et al.*, in *Plasma Physics and Controlled Nuclear Fusion Research* (International Atomic Energy Agency, Vienna, 1991), Vol. 1, p. 453.
[8] E. J. Doyle, R. J. Groebner, and K. H. Burrell *et al.*, Phys. Fluids B **3**, 2300 (1991).
[9] K. Ida, S. Hidekuma, and Y. Miura *et al.*, Phys. Rev. Lett. **65**, 1364 (1990).
[10] R. J. Taylor, M. L. Brown, and B. D. Fried *et al.*, Phys. Rev. Lett. **63**, 2365 (1989).
[11] R. Van Nieuwenhove, G. Van Oost, and R. R. Weynants *et al.*, in *Proceedings of the 18th European Conference on Controlled Fusion and Plasma Physics, Berlin,* (European Physical Society, Petit-Lancey, 1991), Vol. 15C, Part I, p. 405.
[12] S.-I. Itoh and K. Itoh, J. Phys. Soc. Japan **59**, 3815 (1990).
[13] A. B. Hassam, T. M. Antonsen, Jr., J. F. Drake, and C. S. Liu, Phys. Rev. Lett. **66**, 309 (1991).
[14] T. E. Stringer, Phys. Rev. Lett. **22**, 770 (1969).
[15] P. H. Diamond and Y. B. Kim, Phys. Fluids B **3**, 1626 (1991).
[16] F. L. Hinton, Phys. Fluids B **3**, 696 (1991).
[17] F. L. Hinton and G. M. Staebler, Phys. Fluids B **5**, 1281 (1993).
[18] Y. B. Kim, P. H. Diamond, and R. J. Groebner, Phys. Fluids B **3**, 2050 (1991).
[19] P. M. Valanju, M. D. Cavin, R. D. Hazeltine, and E. R. Solano, Phys. Fluids B **4**, 2675 (1992).
[20] W. L. Rowan *et al.*, Phys. Fluids B **4**, 917 (1992).
[21] R. J. Groebner, N. H. Brooks, K. H. Burrell, and L. Rottler, Appl. Phys. Lett. **43**, 920 (1983).
[22] R. J. Groebner, K. H. Burrell, P. Gohil, and R. P. Seraydarian, Rev. Sci. Instrum. **61**, 2920 (1990).
[23] P. Gohil *et al.*, in *Proceedings of the 14th Symposium on Fusion Engineering* (IEEE, New York, 1991).
[24] J. Kim *et al.*, in *Proceedings of the 12th Symposium on Fusion Engineering* (IEEE, New York, 1987), Vol. I, p. 290.
[25] L. L. Lao, H. St. John, R. D. Stambaugh, A. G. Kellman, and W. Pfeiffer, Nucl. Fusion **25**, 1611 (1985).
[26] F. L. Hinton, J. Kim, Y-B. Kim, A. Brizard, and K. H. Burrell, Phys. Rev. Lett. **72**, 1216 (1994).